

INFRARED RECOMBINATION LINES OF HYDROGEN FROM YOUNG OBJECTS IN THE SOUTHERN GALACTIC PLANE

SARA C. BECK¹

School of Physics and Astronomy of the Raymond and Beverly Sackler Faculty of Exact Sciences and the Wise Observatory,
 Tel-Aviv University, Ramat Aviv, Israel 69978

JACQUELINE FISCHER

Center for Advanced Space Sensing, Naval Research Laboratory, Code 4213.8, Washington, DC 20375

AND

HOWARD A. SMITH²

Laboratory for Astrophysics, National Air and Space Museum 3726, Smithsonian Institution, Washington, DC 20560

Received 1990 July 30; accepted 1991 June 14

ABSTRACT

We have observed near infrared recombination lines of hydrogen in twelve young objects in the southern Galactic plane. The sample includes Herbig-Haro objects and *IRAS* dark cloud point sources from the 1987 catalog of Persson and Campbell. In four of the *IRAS* sources we have measured two or three infrared lines, and their intensity ratios are consistent with models of optically thick ionized winds. The intrinsic line shapes, which we retrieve from maximum entropy deconvolutions, indicate gas velocities of 100 km s^{-1} or more as expected from ionized winds. These sources are apparently embedded pre-main-sequence objects with outflows. They include some of the brightest known YSOs.

Subject headings: infrared: sources — infrared spectra — stars: pre-main-sequence — stars: winds

1. INTRODUCTION

Pre-main-sequence stars in the dust-embedded stage, commonly called young stellar objects or YSOs, have powerful stellar winds and very high mass-loss rates which have significant effects on their evolution and on the evolution and dynamics of the stellar environment. YSOs can be observationally distinguished from obscured H II regions and other infrared sources by their infrared continuum shape, their very dense ionized winds, and, for those old enough to have influenced their surroundings, by their association with CO outflows and other markers of pre-main-sequence status (e.g., Evans et al. 1988; Myers et al. 1987).

IRAS data have made it possible to search for these objects in a systematic way. Persson & Campbell (1987) performed near-infrared photometry on a set of bright *IRAS* sources in the southern Galactic plane and selected 45 candidate YSOs based on their near-infrared colors. The sources all have $F_{\nu}(12 \mu\text{m}) > 1 \text{ Jy}$, spectra which rise toward longer wavelengths, and are generally not identified with cataloged stars, H II regions or planetary nebulae. Nevertheless, most are associated with red optical sources and many with optical nebulosities. We have observed five of these candidate sources in the Br α , Br γ , and/or Pf γ recombination lines of hydrogen (wavelengths 4.05, 2.17, and 3.74 μm , respectively). We selected sources for which possible recombination line emission appeared in the CVF spectra of Persson and Campbell; the shapes and relative intensities of the infrared lines are well-established discriminants between YSOs and other infrared sources, and also provide much infor-

mation on outflow structure and conditions in the inner ionized zone. Two or three of the infrared lines were detected in four of the sources, and it is on these four that this paper concentrates.

In the following section we discuss the individual sources. The *IRAS* 100 μm sky flux plate images of the *IRAS* sources are shown in Figure 1 (Plates 7–10). The gray scale plots were made from the Galactic plane images distributed by IPAC. Distance is the key parameter in estimating luminosity and mass loss rates. We have estimated distances to the *IRAS* sources from the distances of H II regions or molecular clouds that seem, based on the morphology seen in the *IRAS* sky flux plates, to be associated with the YSO. Objects used for distance indicators are marked on Figure 1. Kinematic distances were derived using Brand's (1986) rotation curve, $\theta(\text{km s}^{-1})/220 = (R[\text{kpc}]/8.5)^{0.0362}$.

IRAS 07173–1733 ($l = 231^{\circ}80$, $b = -01^{\circ}97$).—This object can be tentatively identified with the 13.5 mag H α emission star DW CMa at $\alpha = 07^{\text{h}}17^{\text{m}}22^{\text{s}}.2$, $\delta = -17^{\circ}33'42''$. The ^{12}CO surveys of Dame et al. (1987) and May, Murphy, & Thaddeus (1988) found a large molecular cloud encompassing this source. That cloud has a V_{LSR} velocity of 43 km s^{-1} , yielding a kinematic distance of $4 \pm 0.6 \text{ kpc}$. However, the low level far-infrared emission surrounding this source is part of an apparent loop of infrared emission which is centered at $l = 234^{\circ}$, $b = 3^{\circ}$ and has apparent diameter of about 5° . Molecular clouds in this loop have V_{LSR} from 43 km s^{-1} in the Galactic northwest to 19 km s^{-1} in the southeast. In its spatial and velocity structure this loop resembles the starforming loops discussed by Schwartz (1987). If this region is in fact a loop, the velocities observed are expected to be projected velocities of an expanding shell, and the appropriate velocity for distance estimates is the centroid, 31 km s^{-1} , which corresponds to 2.75 kpc and would put the source in the Orion arm. We have therefore estimated the distance to this source to be

¹ Visiting International Fellow, Laboratory for Astrophysics, National Air and Space Museum

² Visiting Astronomer at the Cerro-Tololo Inter-American Observatory, operated by the Association of Universities for Research in Astronomy under contract with the National Science Foundation

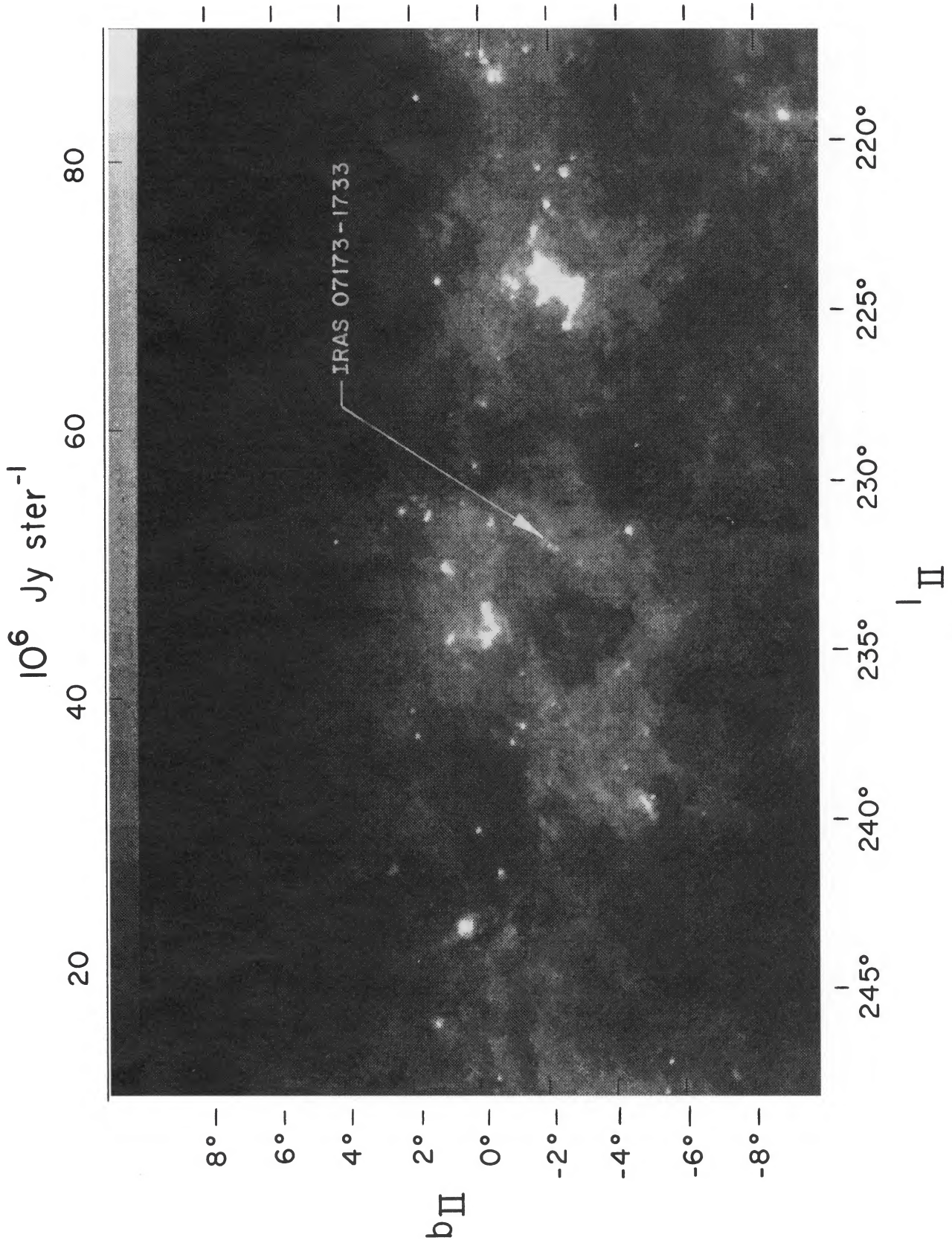


FIG. 1a

FIG. 1.—Gray scale plots of the 100 μm IRAS sky flux image fields, in Galactic coordinates, for the IRAS YSO sources with detected recombination lines. The gray scale levels are displayed in wedges at the top for each image. The positions of the YSO sources and the distance indicator(s) used for each source are indicated by arrows. (a) IRAS-07173-1733, (b) IRAS 09014-4736, (c) IRAS 12389-6147, (d) IRAS 13481-6124.

BECK, FISCHER, & SMITH (see 383, 336)

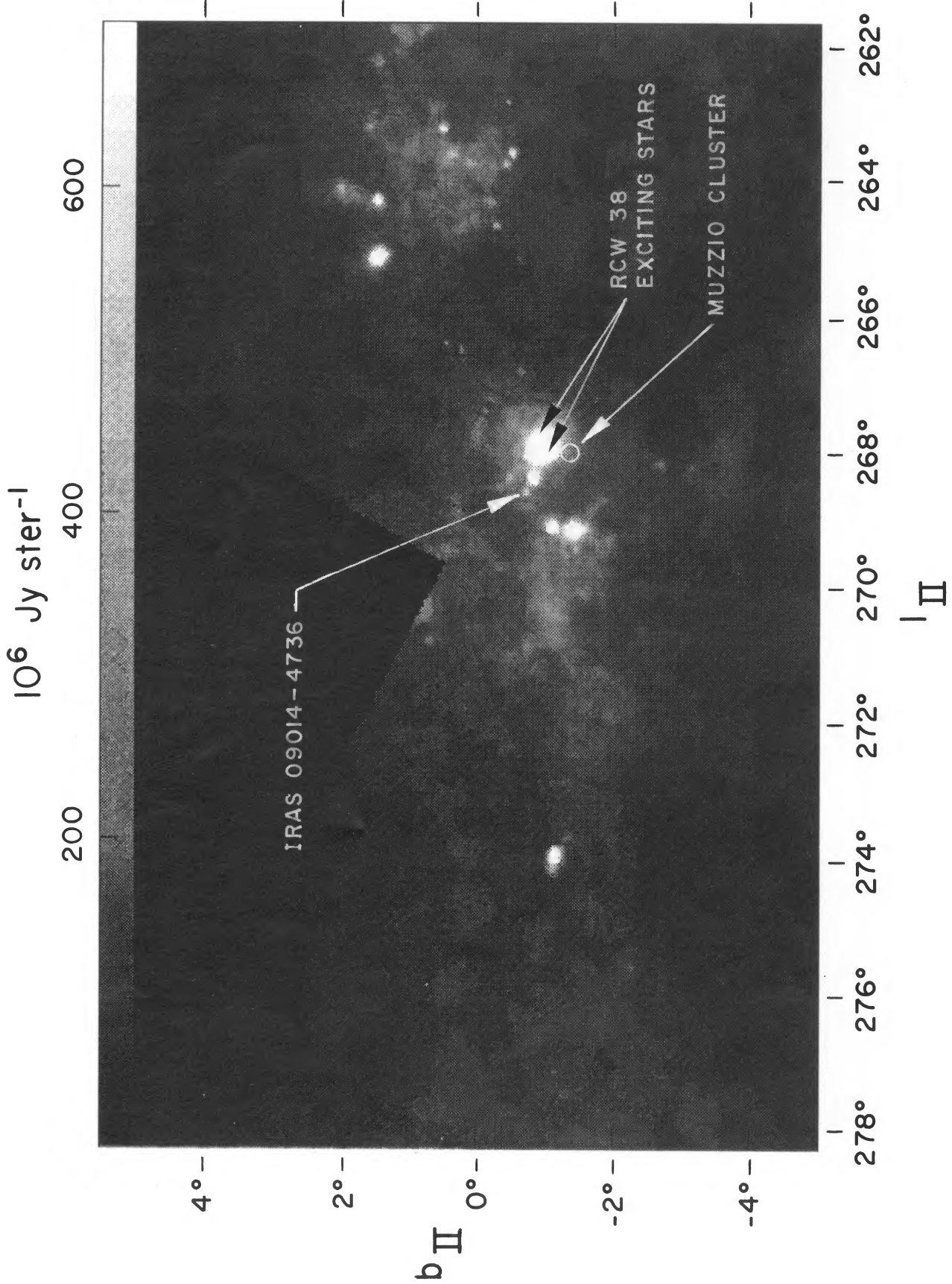


FIG. 1b

BECK, FISCHER, & SMITH (see 383, 336)

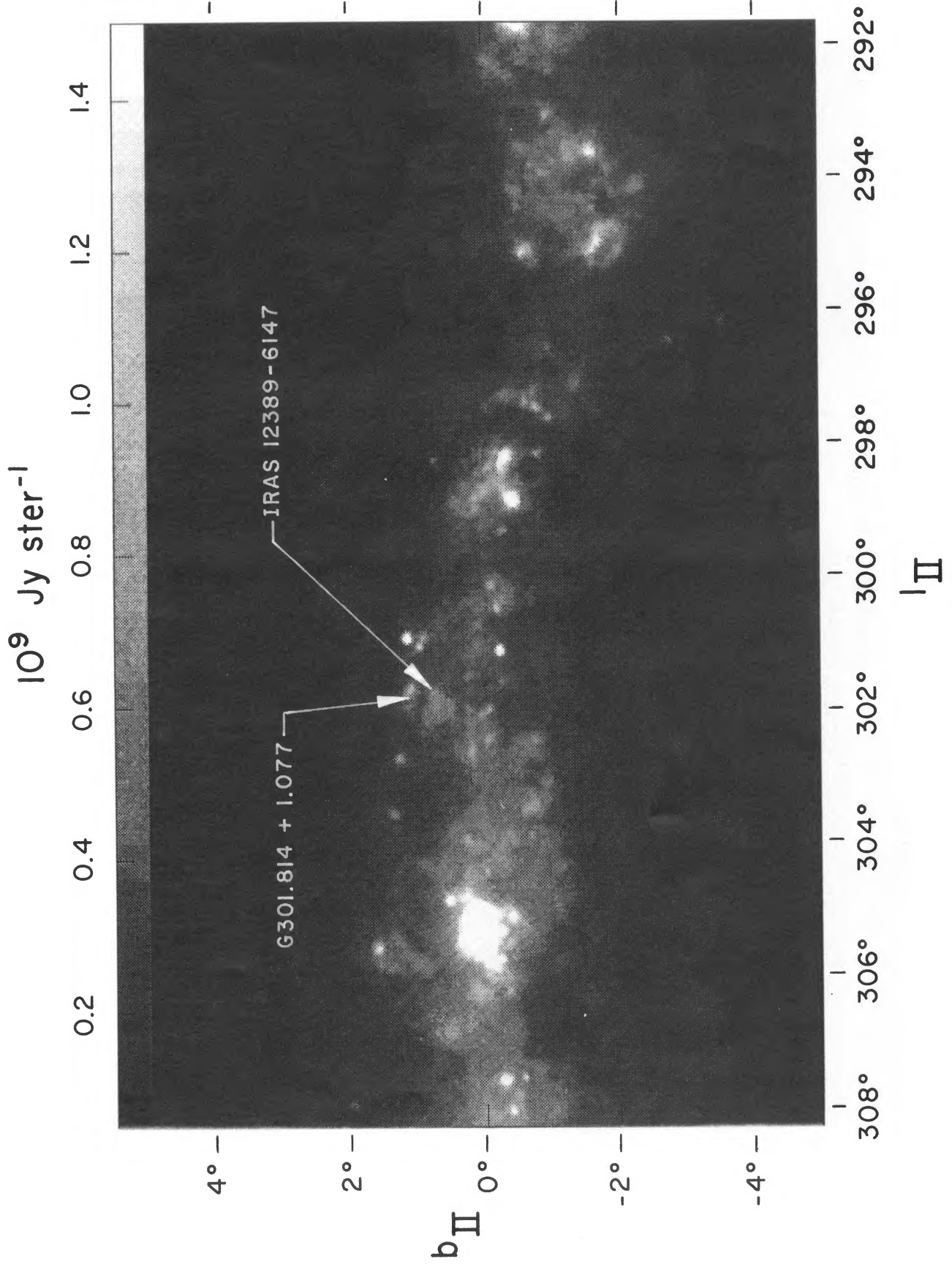


FIG. 1c

BECK, FISCHER, & SMITH (see 383, 336)

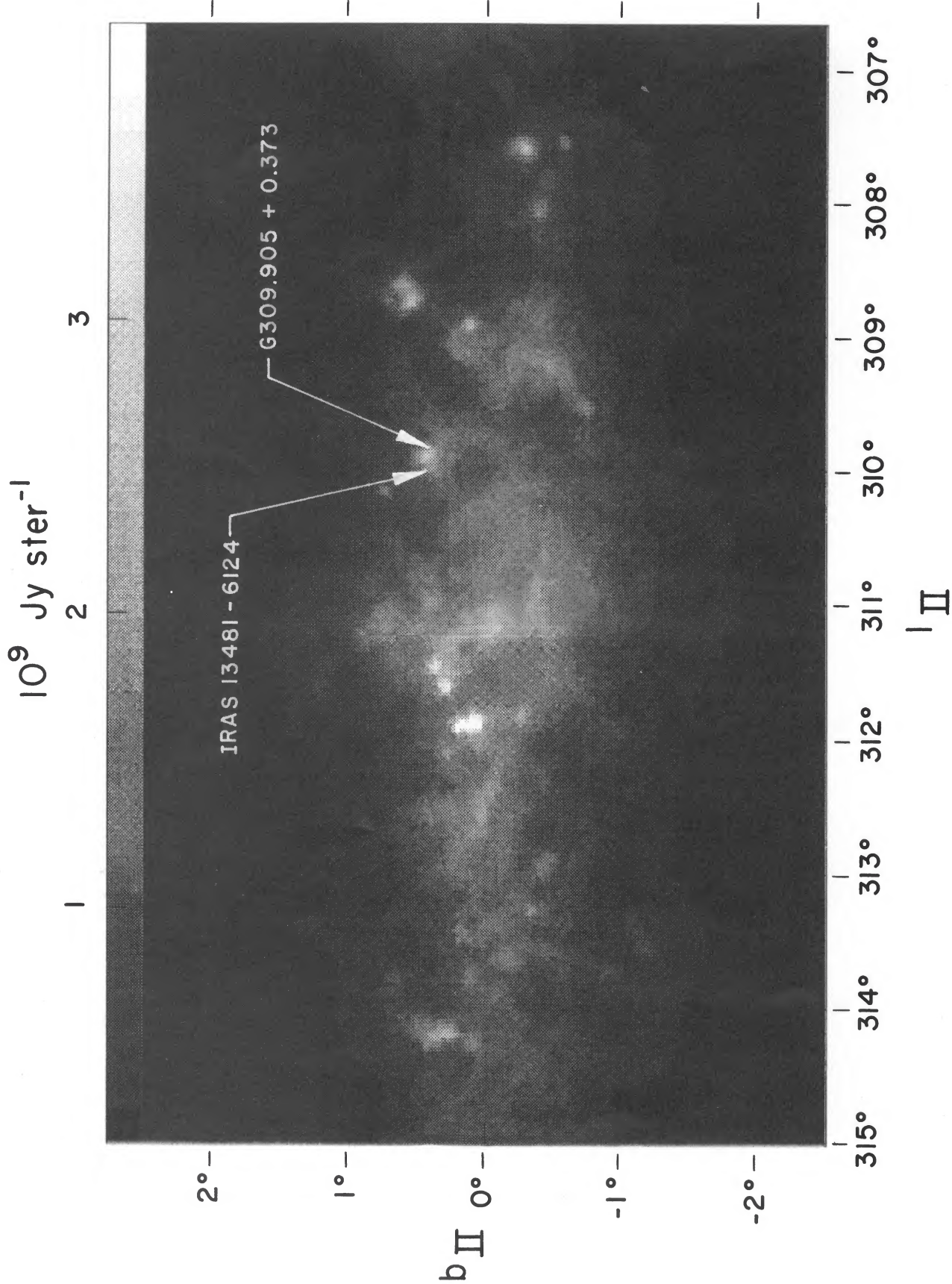


FIG. 1d

BECK, FISCHER, & SMITH (see 383, 336)

2.75 ± 1.25 kpc, where the uncertainties reflect the velocity spread in the loop.

IRAS 09014–4736 ($l = 268^\circ.62$, $b = -00^\circ.74$).—Wouterloot & Brand (1989) found two velocity components for the source, for which we derive kinematic distances of 1.35 or 2.61 kpc. However, at the Galactic longitude of this source small velocity differences create large distance uncertainties: the random velocity dispersion of molecular clouds, ± 6 km s⁻¹, corresponds to about ± 1.3 kpc. We have therefore used photo-metrically derived distance estimates. In Figure 1b it may be seen that extended 100 μ m emission envelopes both the *IRAS* source and a young OB cluster (Muzzio 1979) associated with RCW 38 (Rodgers, Campbell, & Whiteoak 1960). Muzzio derived a photometric distance of 1.7 kpc to the cluster. In his 1985 study of the Vela ridge Murphy (1985) considered CO structure and photometric distance indicators and concluded that the ridge lies at a distance of 1.6 ± 0.8 kpc. In this work we have adopted 1.7 ± 0.9 kpc for *IRAS 09014–4736*.

IRAS 12389–6147 ($l = 301^\circ.82$, $b = 00^\circ.78$).—This source may be connected in a loop structure with G301.814+1.077, an optical H II region about 18' away, but the association is uncertain. Based on the -42 km s⁻¹ velocity Caswell & Haynes (1987) found for that source, and the kinematic distances of other nearby H II regions, we adopt 4.5 ± 2.5 kpc for the distance to this object.

IRAS 13487–6124 ($l = 310^\circ.02$, $b = 00^\circ.39$).—Extended 100 μ m emission connects this source with G309.905+0.373, an H II region 7' away which shows two velocities in H₂CO absorption corresponding to distances of 5.5 or 3.4/7.5 kpc. It is interesting to observe that these sources may also be part of a loop. We have adopted a distance of 5.5 ± 2.5 kpc.

In addition to these *IRAS* candidates, we observed a selection of other YSOs and sources associated with Herbig-Haro objects, which are thought to be likely candidates for outflows. Re 4 and Re 5 are nebulae within the larger Gum nebula ($d \approx 450$ pc), a site of recent active star formation, collimated optical jets, and small dense molecular clouds (Graham 1986). Re 4 is a small emission line source (including H α emission) with the low excitation characteristics of an HH object. Re 5 is a nebula whose optical features are a red continuum and some absorption lines, but no emission; nevertheless it contains an infrared source. In both objects spectra were taken centered on the 2 μ m infrared peaks, slightly offset from the optical nebulosity (for Re 4 the infrared source of 0 $^\circ$:34 west of a visible reference star, near the head of the nebulosity; Graham 1986 and J. A. Graham, private communication). HH 46, located in Bok globule Sandqvist 111 in the Gum nebula, has H₂ emission and a broad and asymmetric H α line; we pointed at the IR source at the head of the nebulosity (Graham 1986; Graham & Elias 1983; J. A. Graham, private communication). HH 120, also in the Gum nebula, shows typical shocked emission lines, and the source IRS 4 thought to be responsible for the shocks has a luminosity of $0.9 L_\odot$ (Pettersson 1984). The Schwartz-Henize object is located in the Cha I association at a distance of about 140 pc. It is thought to be a $14 L_\odot$ pre-main sequence object, perhaps a T Tauri star, with a disk seen almost edge on (Cohen & Schwartz 1984). HH57S is located in a dark cloud in the Norma 1 association (Reipurth & Wamsteker 1983; Schwartz 1977). The infrared source responsible for HH 100, in the R CrA dark cloud, has been suggested to be an FU Ori star in the fading stage of a recent flare (Reipurth & Wamsteker 1983). Finally we also observed the Persson and Campbell source *IRAS 14206–6151/1* but did not detect any line emission.

2. OBSERVATIONS AND ANALYSIS

2.1. Observations and Calibration

The observations were made with the Infrared Grating Spectrometer at the CTIO 1.5 m telescope on 1988 March 7, 8, 9, & 10 March. Weather conditions varied from excellent to mediocre, with intermittent thin clouds on one and one-half nights. The beam size was $5'' \times 5''$ at 3.74 and 4.05 μ m and $10'' \times 10''$ at 2.17 μ m. Nether the signal nor the noise changed appreciably with aperture. The spectral resolution was 285 km s⁻¹ at Br γ and 185 km s⁻¹ Br α and Pf γ . The frequency calibration was checked with argon calibration lamp lines and the Brackett lines in the H II G333.6–0.2 (where the lines are known to be about 40 km s⁻¹ wide; Geballe et al. 1981).

Because the Br α and Pf γ data were recorded on some nights with varying weather conditions, we decided it was preferable to use the source continuum, rather than a standard star, for calibration. After examining calibration star data for these nights, we concluded that this was indeed the better method. We therefore found the relative intensity of those lines by taking the observed equivalent width and obtained absolute fluxes from Persson & Campbell's photometric measurements of the continuum flux at the wavelengths of interest. The continuum and line fluxes appear in Table 1A. Br γ was measured under very stable conditions, and Br γ fluxes calibrated with the standard stars G1 347a (SJ 9607; spectral type M5) and G1 390 (SJ 9608; spectral type M0) give results consistent to 20% with the equivalent width method. For consistency, however, we use the fluxes from the equivalent width method for Br γ as well. The uncertainties reflect the uncertainty in determining the continuum levels near the lines. The Pf γ uncertainties are particularly high because the baseline at that wavelength is very noisy, making it hard to measure the continuum. The error bars shown on the first points of the spectra are typical of the variations at each point.

2.2. Extinction Correction

The extinction derived to YSOs can, even in the infrared, have an important effect on the estimated source luminosities, and we therefore consider several methods for deriving the extinction. The preferred method is to compare a pair of lines at widely separated wavelengths for which the intrinsic ratio of line strengths is known. This method is commonly used in H II regions where normal recombination theory holds and suitable line pairs are readily found, but has been less applied to YSOs because the intrinsic line ratios in these objects are less well known. A number of authors have addressed the question of line intensities in YSOs (e.g., Krolik & Smith 1981; Simon et al. 1981). Smith et al. (1987b) develop an analytic model to treat winds with a variety of flow parameters. Their results show that the Br γ /Pf γ ratio is very insensitive to flow details and will for all common cases approximately equal 3.5 (a very similar result was found by Alonso-Costa & Kwan 1989 for their models). We therefore used the Br γ /Pf γ ratio as our basis for calculating the relative extinction, and the resulting absolute extinctions (derived from the relative obscuration using a reddening law) are shown in Table 1B. Since Br γ was not measured in *IRAS 12389–6147* we of necessity used another method to determine the extinction in that source. We attempted to compare the continuum shape to an assumed intrinsic value. This has been applied with success to T Tauri stars (Rydgren 1976) and A0 stars in clouds (Tanaka et al. 1990), but the choice of an assumed intrinsic spectrum is com-

TABLE 1A
 OBSERVED LINE PARAMETERS

NAME	OBSERVED FLUX ^a ($\times 10^{-20} \text{W cm}^{-2}$)			OBSERVED LINE RATIO		CONTINUUM FLUX (Jy)		
	Br α	Br γ	Pf γ	Br α /Br γ	Br α /Pf γ	Br α	Br γ	Pf γ
IRAS 07173–1733	4.0 (1.1)	4.4 (1.3)	1.4 (<2.2)	0.91 (0.38)	2.9 ...	4.6	1.8	4.1
IRAS 09014–4736	6.1 (1.0)	1.5 (0.42)	1.8 (+2.0, –1.2)	4.1 (1.3)	3.4 (+4.1, –2.1)	2.2	0.3	1.8
IRAS 12389–6147	27 (4.6)	...	9.1 (2.7)	...	3.0 (1.1)	9.9	1.9	8.4
IRAS 13481–6124	45 (6.8)	16 (2.4)	17 (6.3)	2.8 (0.56)	2.6 (1.0)	41.0	7.4	34.
HH 46	<5
HH 57S	0.3 (0.06)
HH 100	1.3 (0.20)
HH 120	<7
Schwartz-Henize	<6 (0.2)	1
IRAS 14206–6151/1	<0.5
Re 4	<2
Re 5	<0.2

^a Uncertainties are $\pm 3\sigma$; where the uncertainties are asymmetric, the maximum and minimum 3σ values are given.

 TABLE 1B
 DERIVED PARAMETERS

NAME	A_V (mag)	ΔV (FWHM) (km s^{-1}) ME METHOD ^b			INTRINSIC FLUX ($\times 10^{-20} \text{W cm}^2$)			INTRINSIC LINE RATIOS	
		Br α	Br γ	Pf γ	Br α	Br γ	Pf γ	Br α /Br γ	Br α /Pf γ
IRAS 07173–1733	2	220	240	...	4.2	5.2	1.5	0.81	2.8
IRAS 09014–4736	26	120	110	105	12	14	4.0	0.91	3.1
IRAS 12389–6147	21 ^c	150	...	145	47	...	17	...	2.7
IRAS 13481–6124	24	190	190	...	86	120	36	0.7	2.4

^a Extinction based on fitting line ratios to model (see text).

^b Limitations to the maximum entropy method are discussed in the text.

^c Extinction from the method of Rydgren 1976.

plicated in these *IRAS* sources by the presence of hot dust. We found that for assumed intrinsic spectra like these two categories the corrected fluxes are not very sensitive to the method, and so A_V for IRAS 12389–6147 was found from Rydgren's model.

2.3. Line Shapes and the Maximum Entropy Method

The summed and averaged spectra are displayed in Figure 2. The Br α spectra were divided by an incandescent spectrum to remove variations in sensitivity across the array. The Br γ spectra were divided by that of the standard star Gl 390 to remove atmospheric features and the Pf γ spectra were divided by a spectrum of Sirius in which the strong Pf γ absorption found in that star was replaced by an interpolated continuum. The Pf γ spectra are much noisier than those at the other wavelengths. This is probably due to atmospheric features in the 3.74 μm region and the weather conditions during the observations. Therefore we attempted to analyze and deconvolve only the Pf γ spectra of IRAS 09014–4736 and IRAS 12389–6147.

The profiles of infrared emission lines provide valuable information on the source velocity structure. The resolution of the grating used in these observations is on the order of the

expected source line widths. However, if the spectral transfer function (STF) of the spectrometer is sufficiently well known, it can be deconvolved from the observed spectrum to yield the source spectrum with an effective resolution much higher than the instrumental value. For this work, the lamp and H II region results were used to give the spectral transfer function of the system. While deconvolution is in principle straightforward, if the raw data are noisy simple linear approaches will be problematic. In a recent comparison of deconvolution methods (Naylor, Lermer, & Furniss 1990), the method of maximum entropy (ME) gave results consistently superior to those of other more commonly used methods. While the ME method has been widely used in enhancing the effective spatial resolution of radio and infrared maps, it has not to our knowledge been used before to deconvolve astronomical spectra. The confidence that can be placed in the ME solution depends on how well one knows the STF and the noise characteristics of the raw data. For the Infrared Grating Spectrometer at the 1.5 m telescope, the slit width was narrower than the pixel size though wider than a point source. In this case, the FWHM of the STF is independent of the source extent, and it should therefore not be affected by the source size, although the FWZI

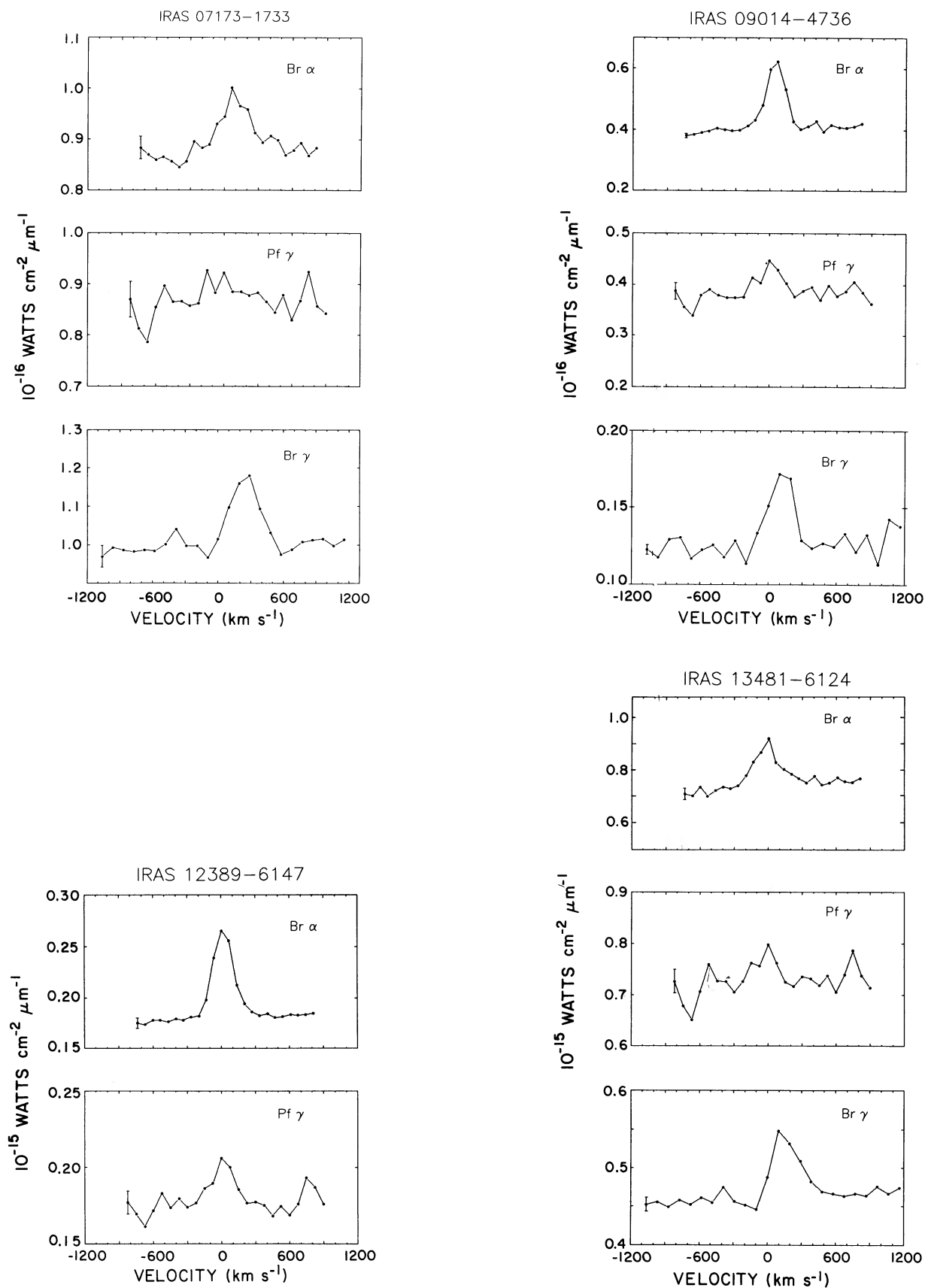


FIG. 2.—The observed spectra, summed and averaged as described in the text. The intensity scale is derived by interpolating the photometry of Persson & Campbell (1987).

TABLE 2
 SOURCE PARAMETERS

NAME	OUTFLOW "s" ^a (1)	T(K) ^b			DISTANCE (kpc)	LUMINOSITY (L_{\odot})	MASS-LOSS RATE ^c ($M_{\odot} \text{ yr}^{-1}$) (3)
		T_1	T_2 (2)	T_3			
IRAS 07173–1733.....	0.8	1460	240	57	2.75 ± 1.25	2.8×10^3	2.8×10^{-7}
IRAS 09014–4736.....	0.5	1360	230	50	1.7 ± 0.9	4.95×10^5	2.0×10^{-7}
IRAS 12389–6147.....	1.3	900	190	41	4.5 ± 2.5	4.7×10^4	2.7×10^{-6}
IRAS 13481–6124.....	1.6	850	190	50	5.5 ± 2.5	1.8×10^5	6.8×10^{-6}

^a Velocity law coefficient, based on the ratio $\text{Br}\alpha/\text{Br}\gamma$, except in the case of IRAS 12389–6147 (see text).

^b Values from a three-temperature fit to the continuum data (see text).

^c Based on a nominal value of $s = 1$ for all sources.

is somewhat broader for extended sources. The result is a slight underestimate of the source FWZI after deconvolution. An additional consideration is that the signal-to-noise ratios of the data in these observations are only fair. The ME method is usually applied to observations of very high signal-to-noise ratio, and the deconvolutions presented here do not display this aspect of the method to its best advantage. However, because the method models the data points as a set, it can extract additional information even from low SNR data. We estimate that the ME method here enhanced the effective spectral resolution only by a factor of approximately 2; a factor of 4 or more should be attainable with data of better signal-to-noise ratio. Better demonstrations of the power of the method, using data specifically obtained for this sort of deconvolution, can be found in Naylor et al.

A further question in any spectral deconvolution (especially for nonlinear methods such as ME) is the reliability and self-consistency of the results. We have checked that the deconvolutions do not return spurious features by reconvolving the deconvolved line with the STF and comparing that to the raw data (to which it should ideally be identical). In Figure the deconvolved $\text{Br}\gamma$ and $\text{Br}\alpha$ spectra and the $\text{P}\gamma$ spectrum of IRAS 12389–6147 are displayed, along with the same spectra reconvolved and overplotted with the raw data. It may be seen that the agreement between the raw data and the data reconvolved with the STF is very good for all the lines. However, the deconvolved $\text{Br}\gamma$ lines all appear to have secondary features at intervals of about 400 km s^{-1} in both directions from the peak. Four such features are clearly seen in all spectra except for IRAS 07173–1733, where two are obvious and one is weak. These features appear in the raw data, which have faint wiggles at these positions which the ME method enhanced. It is not known how these arise, but since they appear identically in all sources we conclude they are artifacts of the spectrometer. The $\text{Br}\alpha$ and $\text{P}\gamma$ results are free of this problem.

The FWHM of the deconvolved spectra are listed in Table 1B. We estimate the accuracy of the FWHM values to be $\pm 35 \text{ km s}^{-1}$ and $\pm 50 \text{ km s}^{-1}$ at $\text{Br}\alpha$ and $\text{Br}\gamma$, respectively. The narrowest lines were in IRAS 09014–4736, for which we formally find widths of about 110 km s^{-1} for all its lines. This is approximately equal to the ME-enhanced resolution and the lines in IRAS 09014–4736 may not be resolved. The other sources have obviously wider lines. Other details of the line shapes, such as the apparent wings on the IRAS 07173–1733 spectra, are more susceptible to imprecision in the knowledge of the STF, and should be confirmed. In no source is there evidence for double peaks or other complex structure. Within each source the deconvolved widths of the different lines are equal to within our measurement accuracy.

3. RESULTS AND DISCUSSION

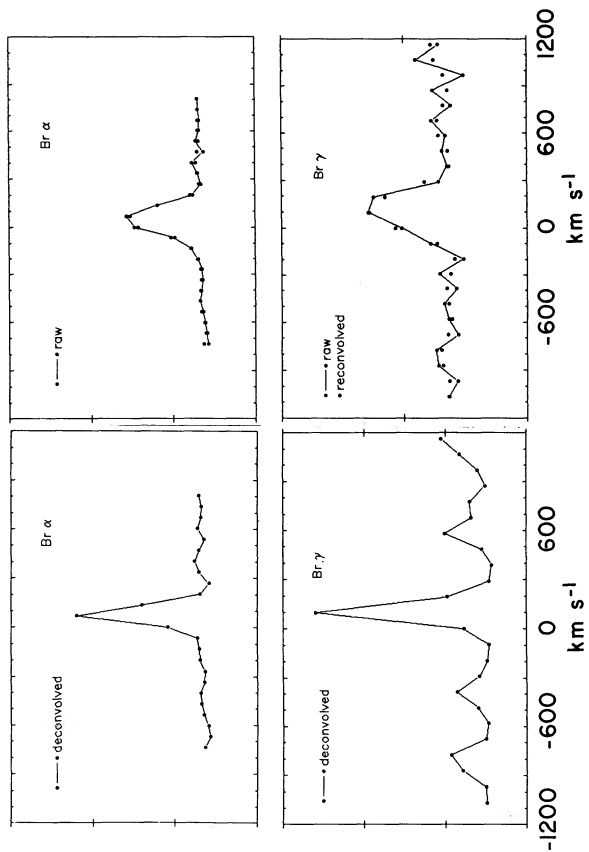
3.1. The Nature of the IRAS Sources

The evidence is strong that these sources are in fact YSOs. Persson & Campbell (1987) argue convincingly that the IR continua of these objects are typical of YSOs and not of H II regions or late-type stars, with the possible exception of IRAS 14206–6151/1 which has a double-peaked spectral shape. We present here two spectroscopic diagnostics: the hydrogen recombination line ratios, and the line shapes. The ratios of the infrared lines are quite inconsistent with optically thin "Case B" recombination (for which $\text{Br}\alpha/\text{Br}\gamma = 2.86$, $\text{Br}\alpha/\text{P}\gamma = 7.1$) and the line shapes show very high velocity motions, with emission extending to several hundred km s^{-1} . Both are typical of the dense ionized winds from YSOs. We note that we did not detect $\text{Br}\gamma$ line emission in IRAS 12406–6151/1, although its presence is suggested in the CVF spectrum of Persson and Campbell.

We next derive the parameters of the outflows based on models of YSO winds. YSO outflows have been modeled for a wide variety of conditions of ionization, optical depth, and spatial structure by Smith et al. (1987b),³ Simon et al. (1983), Hamann & Simon (1987), and others. These models predict the ratios of line intensities ($\text{Br}\alpha/\text{Br}\gamma$ and $\text{Br}\alpha/\text{P}\gamma$) for different outflow structures. In Figure 4a the observed line ratios are plotted for a selection of YSOs including the sources discussed here. The solid line in the figure shows the locus of points of the intrinsic ratios as a function of the outflow parameter s , where $v(r) = v_0(r/r_0)^s$ according to the models of Smith et al. (1987b). In Figure 4b the line ratios corrected for extinction are plotted, and the theoretical points for sample values of s are marked. For sources taken from the literature the extinction derived by the original authors was used. It is clear that the corrected ratios are in good agreement with the analytic models. Values of s are listed in Table 2 and range from 0.5 (weak acceleration) to 1.6 (moderate acceleration). The uncertainties of the fluxes are, however, reflected in the determination of s , as may be seen in the figure. Line widths can be used to corroborate model implications derived from intensity ratios. Since lines with higher optical depths are seen coming from larger distances from the star, the widths of the different lines are in theory related to the velocity structure of the flow. Our derived FWHM values are approximately equal for both Brackett lines in each source. More accurate and higher velocity resolution observations are needed for more precise modeling. The analy-

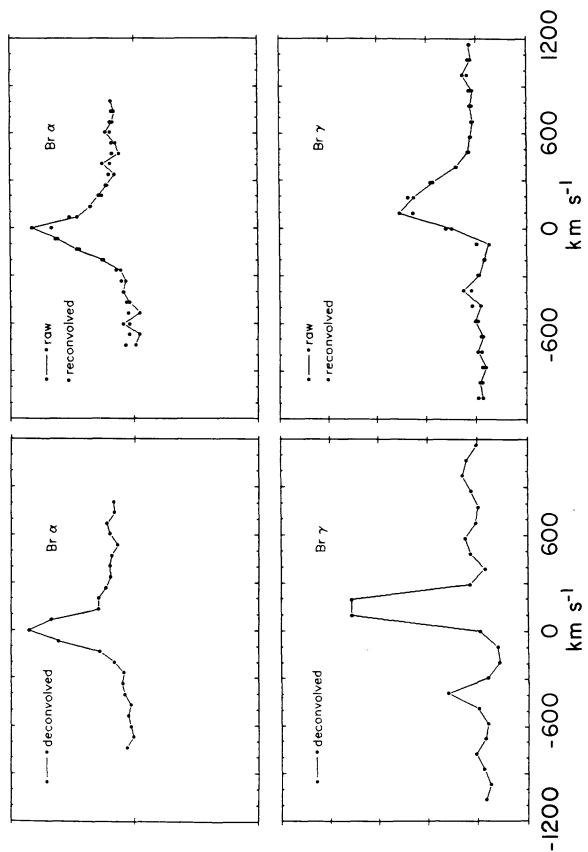
³ There is an error in the numerical coefficient in eq. (17) in this paper. The correct expression is $F(\text{Br}\alpha)/F(\text{P}\gamma) = 0.8 \times 12.90^{(2+s)/3(s+1)}$.

IRAS 09014-4736



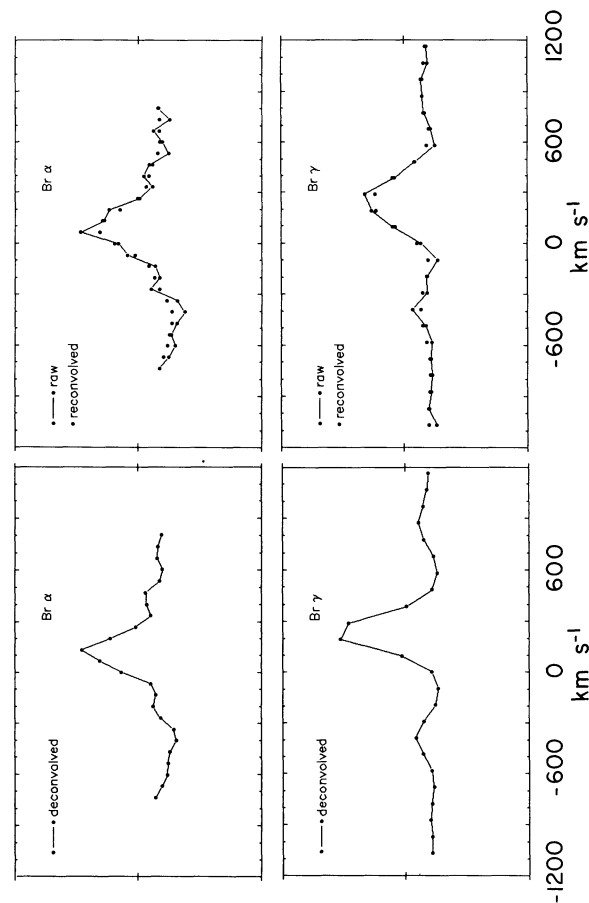
MAXIMUM ENTROPY SOLUTION

IRAS 13481-6124



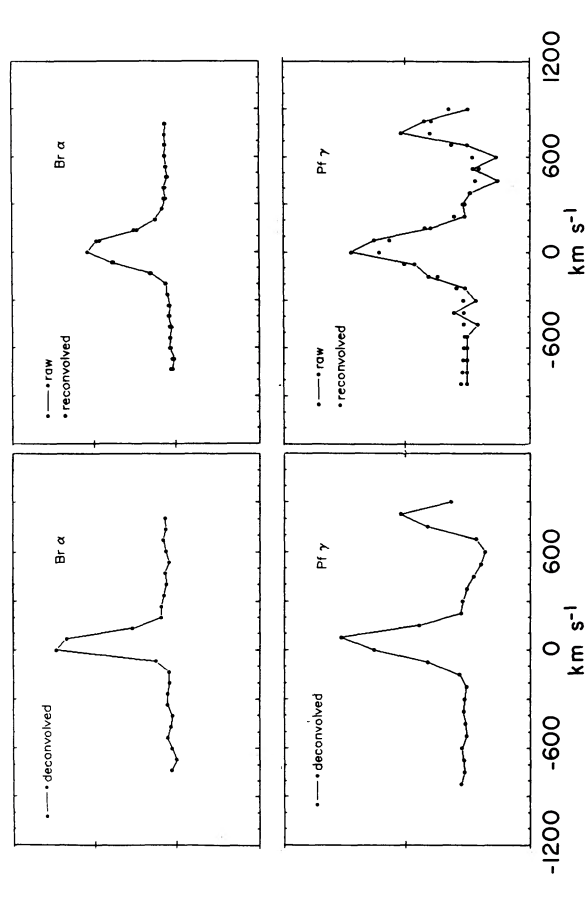
MAXIMUM ENTROPY SOLUTION

IRAS 07173-1733



MAXIMUM ENTROPY SOLUTION

IRAS 12389-6147



MAXIMUM ENTROPY SOLUTION

FIG. 3.—In each part of the figure, the left-hand panels show the observed Br γ and Br α spectra deconvolved by the maximum entropy method, and the right-hand panels show the deconvolved spectra which have been reconvolved with the STF (solid lines) and overplotted with the raw data (dots). Intensity scales are arbitrary.

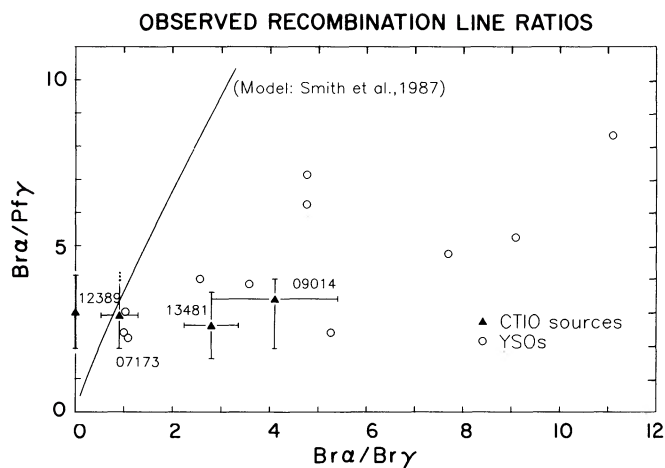


FIG. 4a

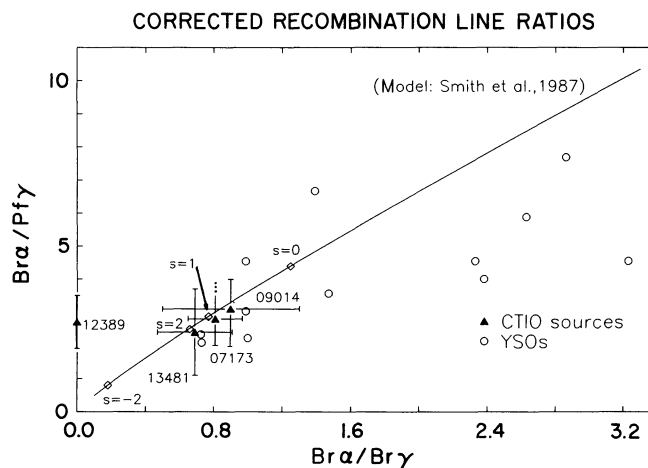


FIG. 4b

FIG. 4.—The $\text{Br}\alpha/\text{Br}\gamma$ and $\text{Br}\alpha/\text{P}\gamma$ line ratios observed (a) in the sources and (b) extinction-corrected to fit the theoretical model. Open circles are sources from the literature, and triangles are the *IRAS* sources discussed here. The expected values for outflows with velocity structure $v \propto r^s$ are shown as the solid line. There was no $\text{Br}\gamma$ observation for 12389–6147, so the possible range of ratios is shown on the left axis. The open diamonds are the theoretical points for s equal to (from top right to lower left) 0, 1, 2, and -2 .

tic model of Smith et al. makes several approximations, is not valid around the point $s = -1$, and addresses only the line intensities. The model has recently been extended with a computer model of the outflow and line shapes (L. Cassar 1989, private communication) based on the original algorithms of Simon et al. (1981). The analytic and more exact computed models agree in their predictions of line intensities and flow parameters and will be discussed in a separate paper (Cassar, Fischer, & Smith 1992).

The infrared continua of YSOs are emitted by dust at a range of characteristic temperatures corresponding to different distances from the star. To derive the luminosities we fit the continua to blackbodies at the three temperatures found from the $1.25/2.2 \mu\text{m}$, $12/25 \mu\text{m}$, and $60/100 \mu\text{m}$ colors. The temperatures are listed in Table 2. The integrated luminosities of each source at the assumed distances are obtained by color-correcting the *IRAS* data and integrating under a composite blackbody curve as described in Mozurkewich, Schwartz, & Smith (1986) and are also shown in Table 2. The uncertainty of the distances adopted for the YSOs results in a corresponding uncertainty in the total luminosity, but even so it can be seen that all of the YSOs observed are fairly bright, and *IRAS* 12389–6147 and *IRAS* 13418–6124 may, if at their farthest distances, be among the most luminous YSOs known. The luminosity does not seem to correlate with dust temperatures, line widths, or extinction, nor do the temperatures show any correlation with the other parameters. *IRAS* 07173–1733 and *IRAS* 09014–4736 are similar in temperature in spite of their great differences in extinction, and *IRAS* 09014–4736 and *IRAS* 13481–6124 have similar extinction and quite different temperatures. This disagrees with the simple and common finding that the most obscured sources are the coldest and may relate to the submicron appearance of these YSOs which will be discussed in § 3.2, below.

In conclusion, we have shown that the observed *IRAS* sources are luminous YSOs with dense ionized winds, fairly hot near infrared temperatures, and a variety of outflow characteristics.

3.2. *IRAS* Source Associations with Submicron Sources

All the YSOs observed are very highly obscured ($A_v \geq 10$) except *IRAS* 07173–1733 which is moderately obscured. The

finding of Persson and Campbell that all except *IRAS* 13481–6124 are associated with red nebulosities is therefore unexpected. There are several possible explanations. First, as the YSOs are in crowded fields, the apparent association with nebulosity may be coincidental. Second, if the obscuring material is not uniform but has holes then the nebulosity may be escaped outflow gas or circumstellar material illuminated by light from the hidden YSO seen through the holes. Further evidence that the extinction is irregular, permitting the YSO to be observed at much shorter wavelengths than would be expected, comes from the submicron spectroscopy of Persson & Hamann (1990). They found that *IRAS* 07173–1733 has strong emission from the infrared Ca II triplet, O I, and several high-level Paschen lines of hydrogen (consistent with its identification with DW CMa), that *IRAS* 12389–6147 has weak Paschen lines and Ca II emission and strong O I emission, and that *IRAS* 09014–4836 has very strong O I emission and hints of Ca II emission and Paschen line absorptions. These spectra are characteristic of young stars with winds, such as T Tauri or Ae/Be stars, but cannot be classified further because of the notorious variety of spectral features in such stars. The submicron lines are expected to arise in gas much less dense than that responsible for the optically thick infrared recombination lines and therefore probe the wind that has expanded to a much larger distance from the star (some hundreds of AU, if a typical Ae/Be or T Tauri wind, compared to about 0.75 AU for the infrared lines). The submicron spectra confirm that the *IRAS* sources are very young stars and that the extinction is sufficiently irregular that the short wavelength light can be seen either directly or after scattering. These obscuration irregularities may complicate or mislead attempts to find the distribution of dust and dust temperature in these sources with simple spherically symmetric models.

3.3. Derivation of Mass-Loss Rates

We estimate the mass loss rates for the *IRAS* sources using equation (3) of Smith et al. (1987b) and list them in Table 2. They are fairly high, ranging from a few times 10^{-7} to several times $10^{-6} M_{\odot} \text{ yr}^{-1}$ consistent with the high luminosity of these sources. Three of the other sources observed have positive detections of one of the recombination lines. The mass-loss rates of HH 100 and the Schwartz-Henize object are estimated

assuming a representative flow with $s = 0$ and $v = 100 \text{ km s}^{-1}$ and are about $10^{-9} M_{\odot} \text{ yr}^{-1}$, consistent with what would be seen from an early-type T Tauri star. The null detections in the other sources are consistent with their estimated distances and total luminosities and the approximate analytic relation between luminosity and line flux derived by Smith et al. (1987a). The observations and limits are in reasonable agreement with the predictions for sources where the distances and extinctions have been estimated.

4. CONCLUSIONS

This project was undertaken as a study of a new sample of possible YSOs. We have confirmed that these candidates from the list of Persson & Campbell (1987) are YSOs, among the most luminous known, with some interesting individual aspects:

1. IRAS 07173–1733 is the hottest and least obscured source we observed, has the widest lines, and the submicron spectrum of a young star with a wind. It therefore seems to be the most evolved of the sources observed and is probably relatively close to emerging from its natal cloud and becoming a normal young star.

2. IRAS 09014–4736 has high extinction and the narrowest lines of the modeled sources. We suggest it is at an early stage of its wind activity. The optical lines seen from this source and its fairly high temperature can both be explained if there are

holes in the obscuration through which short-wavelength emission is escaping.

3. IRAS 12389–6147 has line widths and extinction suggestive of an evolutionary state between IRAS 07173–1733 and IRAS 09014–4736. This is consistent with its association with a submicron nebulosity and a T Tauri of Ae/Be star spectrum, suggesting that the obscuration is irregular.

4. IRAS 13481–1624 resembles IRAS 12389–6147 in extinction and line width but not in outflow parameter. It is the only one of the sources with no associated optical nebulosity and may have a more uniform distribution of extinction than do the other YSOs.

These highly obscured YSOs with winds are important as examples of the relationship between outflows and circumstellar material. Comparing our measured line flux ratios to analytic models, we determine the extinctions, and find evidence for wind acceleration in these sources. Future high spectral resolution observations can be used to extend these results.

We thank D. Naylor and N. Lerner for their help with the maximum entropy method, while they were in residence at the Laboratory for Astrophysics. We also thank S. E. Persson and F. Hamann for communicating results to us in advance of publication and T. Dame, D. Murphy, J. Elias, L. Cassar, and J. Graham for helpful discussions. S. C. B. thanks the Smithsonian Institution for a Visiting International Fellowship. This work was supported in part by NASA grant NAGW-1711.

REFERENCES

- Alonso-Costa, J. L., & Kwan, J. 1989, *ApJ*, 338, 403
 Brand, J. 1986, Ph.D. thesis, University of Leiden
 Cassar, L., Fischer, J., & Smith, H. A. 1992, in preparation
 Caswell, J. L., & Haynes, R. F. 1987, *A&A*, 171, 261
 Cohen, M., & Schwartz, R. D. 1984, *AJ*, 89, 277
 Dame, T. M., et al. 1987, *ApJ*, 322, 706
 Evans, N. J., II, Levreault, R. M., Beckwith, S., & Skrutskie, M. 1987, *ApJ*, 320, 364
 Geballe, T. R., Wamsteker, W., Danks, A. C., Lacy, J. H., & Beck, S. C. 1981, *ApJ*, 247, 130
 Graham, J. A. 1986, *ApJ*, 302, 353
 Graham, J. A., & Elias, J. H. 1983, *ApJ*, 272, 615
 Hamann, F., & Simon, M. 1987, *ApJ*, 318, 356
 Krolik, J. H., & Smith, H. A. 1981, *ApJ*, 249, 623
 May, J., Murphy, D. C., & Thaddeus, P. 1988, *A&A*, 73, 51
 Muzurkewich, D., Schwartz, P. R., & Smith, H. A. 1986, *ApJ*, 311, 371
 Murphy, D. C. 1985, Ph.D. thesis, Massachusetts Institute of Technology
 Muzzio, J. C. 1979, *AJ*, 84, 639
 Meyers, P. C., Fuller, G. A., Mathieu, R. D., Beichmann, C. A., Benson, P. J., Schild, R. E., & Emerson, J. P. 1987, *ApJ*, 319, 340
 Naylor, D., Lerner, N., & Furnis, D. 1990, *Appl. Optics*, in press
 Persson, S. E., & Campbell, B. 1987, *AJ*, 94, 416
 Persson, S. E., & Hamann, F. 1990, private communication
 Pettersson, B. 1984, *A&A*, 139, 135
 Reipurth, B., & Wamsteker, W. 1983, *A&A*, 119, 14
 Rodgers, A. W., Campbell, C. T., & Whiteoak, J. B. 1960, *MNRAS*, 121, 103
 Rydgren, A. E. 1976, *PASP*, 88, 111
 Schwartz, P. R. 1987, *ApJ*, 320, 258
 Schwartz, R. D. 1977, *ApJS*, 35, 161
 Simon, M., Felli, M., Cassar, L., Fischer, J., & Massi, M. 1983, *ApJ*, 266, 623
 Simon, M., Righini-Cohen, G., Felli, M., & Fischer, J. 1981, *ApJ*, 245, 552
 Smith, H. A., Fisher, J., Geballe, T. R., Muzurkewich, D., & Schwartz, P. R. 1987a, in *Star Forming Regions*, ed. M. Peimbert & J. Jugaku (Dordrecht: Reidel), 343
 Smith, H. A., Fischer, J., Geballe, T. R., & Schwartz, P. R. 1987b, *ApJ*, 316, 265
 Tanaka, M., Sato, S., Nagata, T., & Yamamoto, T. 1990, *ApJ*, 352, 724
 Wouterloot, J. G. A., & Brand, J. 1989, *A&AS*, 80, 149